# INVESTIGATIONS INTO THE PHOTOACOUSTIC TECHNIQUE FOR OBTAINING OPTICAL ABSORPTION SPECTRA OF SOLIDS

APPROVED:

# INVESTIGATIONS INTO THE PHOTOACOUSTIC TECHNIQUE FOR OBTAINING OPTICAL ABSORPTION SPECTRA OF SOLIDS

by

EMMET MICHAEL MONAHAN, JR., B.S.

THESIS

Presented to the Faculty of the Graduate School of

The University of Texas at Austin

in Partial Fulfillment

of the Requirements

for the Degree of

MASTER OF ARTS

THE UNIVERSITY OF TEXAS AT AUSTIN

January 1975

# A C K N O W L E D G M E N T S

The author wishes to thank Dr. A. W. Nolle for his patient supervision and sage advice during the course of this research.

For the loan of several important pieces of equipment, the author wishes to thank Dr. G. Fredericks and Dr. D. Gavenda.

For the sample of Amorphous $As_2S_3$, the author is grateful to Mr. B. Joiner.

For many helpful discussions on this effort and on many other topics, the author wishes to thank Mr. R. Tropp.

E.M.M.

The University of Texas
at Austin
August 1974

# TABLE OF CONTENTS

# LIST OF ILLUSTRATIONS

# INTRODUCTION

At the Spring 1973 Meeting of the American Physical Society, A. Rosencwaig (March 1973) presented a paper that brought renewed interest to the photoacoustic technique for obtaining the absorption spectra of solids. In a simple picture, the technique measures the temperature rise at the surface of a powder as it absorbs periodic bursts of light. This temperature rise is detected by detecting the corresponding periodic pressure rise in a volume of gas in contact with the powder. As the absorption coefficient increases, the amount of energy absorbed increases; and thus the peak pressure is greater.

The major advantage of this technique is that it uses powders and thus does not require wafers or thin films to be prepared. The photoacoustic technique can also give the absorption spectra of substances such as blood, spectra which are difficult to obtain by more conventional techniques. A major disadvantage of it for studying crystals is the inability to distinguish absorption along a particular crystal axis.

This study will describe a spectrometer that was constructed employing the photoacoustic technique, and it will present a mathematical model for it. It will also present some data in support of the model. This data shows the dependence of the output voltage on the chopping frequency, the gas, the gas pressure, the incident light intensity and the absorption coefficient.

## THEORY

A diagram of the photoacoustic cell that was used is shown in Figure 1. There are two cavities, a sample cavity and a microphone cavity, connected by a small tube. The powder is contained in the lower part of the sample cavity. The chopped light shines down onto the powder through the transparent top of the sample cavity. The diaphragm of a microphone forms one wall of the microphone cavity.

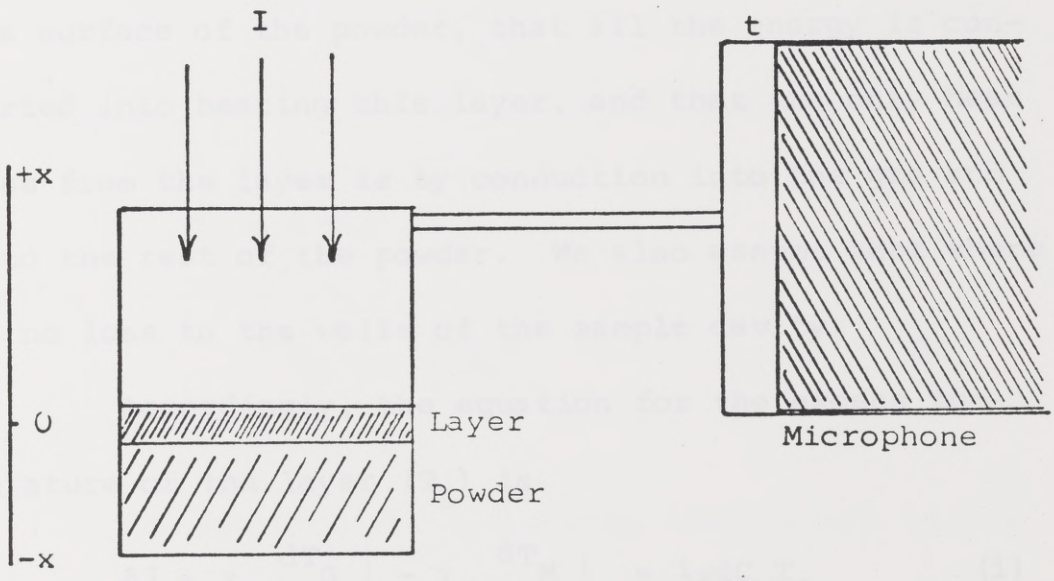


Figure 1. Diagram of Photoacoustic Cell.

The analysis of the acoustic system is in two parts. First, the pressure rise in the sample cavity will be calculated as if it were isolated. The analysis for this was adapted from a discussion by Parker (1973). The pressure at the microphone diaphragm will then be determined by considering an electrical analogy.

Pressure

The model we are using assumes a one-dimensional picture and that all the variables are periodic in time, e.g., $P = P_o + p_e \exp(i\omega t)$. We further assume that all the light is absorbed uniformly in a very thin layer at the surface of the powder, that all the energy is converted into heating this layer, and that the only heat loss from the layer is by conduction into the gas and into the rest of the powder. We also assume that there is no loss to the walls of the sample cavity.

Accordingly, the equation for the excess temperature of the layer ($T_L$) is

$$\beta I + \chi_G \frac{dT_G}{dx}\Big|_o - \chi_M \frac{dT_M}{dx}\Big|_o = i\omega d C_M T_L \qquad (1)$$

where $\beta$ = fraction of incident light absorbed in the layer

$I$ = incident light intensity per unit area

$\chi_G$ = thermal conductivity of gas

$\chi_M$ = thermal conductivity of powder

$d$ = thickness of layer

$C_M$ = specific heat of powder per unit volume

The difference in sign between the second and third term is a result of taking the layer as the origin ($x = o$).

The equation for the excess temperature of the powder ($T_M$) is given as

$$-\chi_M \frac{d^2 T_M}{dx^2} + i\omega C_M T_M = 0 \qquad (2)$$

The meaningful solution of (2) can be written

$$T_M = A \exp (k_M x)$$

where

$$k_M = \left(\frac{i\omega C_M}{\chi_M}\right)^{\frac{1}{2}} \qquad (3)$$

The equation for the excess temperature of the gas ($T_G$) is, from conservation of energy,

$$-\chi_G \frac{d^2 T_G}{dx^2} + i\omega C_p T_G = i\omega p_e a \qquad (4)$$

where $C_p$ = specific heat of the gas at constant pressure per unit volume

$$a = C_p \frac{T_o}{P_o} \left(1 - \frac{1}{\gamma}\right)$$

and $\gamma = C_p / C_v$

We assume an ideal gas equation of state

$$MP = \rho RT \tag{5}$$

where $M$ = grams/mole

and $R$ = gas constant

In this assumption "a" in Equation (4) is one.

From the continuity equation

$$-\frac{\partial \rho}{\partial t} = \rho_o \frac{\partial u}{\partial x}$$ $u$ = particle velocity, and the equation of motion

$$\frac{\partial u}{\partial t} = \frac{1}{\rho} \frac{\partial P}{\partial x}$$

we have that $\frac{d^2 pe}{dx^2} = -\omega^2 \rho_e$ . (6)

From Equation (5)

$$\rho_e = \frac{M}{RT} \left(p_e - \frac{\rho R}{M} T_G\right) \tag{7}$$

The velocity of sound for an ideal gas is

$$c = \left(\frac{\gamma RT}{M}\right)^{\frac{1}{2}} \tag{8}$$

Applying $\frac{d^2}{dx^2}$ to Equation (4) and using Equations (6), (7) and (8), one obtains

$$i\frac{\chi_G}{\omega}\frac{d^4T_G}{dx^4} + \left[C_p + \frac{i\gamma\omega\chi_G}{c^2}\right]\frac{d^2T_G}{dx^2} + C_p\frac{\omega^2}{c^2} = 0 \tag{9}$$

The solution to Equation (9) may be expressed as

$$T_G = B\exp(-ik_G x) + C\exp(ik_G x) + D\exp(-k_2 x)$$

where $k_G = \frac{\omega}{c}$

and $k_2^2 = -\frac{\omega C_p}{i\chi_G} + \frac{\omega^2}{c^2}(1-\gamma)$

Since $\frac{\omega}{c^2} << \frac{C_p}{\chi_G}$

$$K_2 \cong \left(\frac{i\omega C_p}{\chi_G}\right)^{\frac{1}{2}}$$

Substituting this result into Equation (4), one obtains with a high degree of accuracy that

$$pe = C_p[B\exp(-ik_G x) + C\exp(ik_G x)] + d_1 D\exp(-k_2 x) \tag{10}$$

where $d_1 = -i(\gamma-1)\frac{\omega\chi_G}{c^2}$

To evaluate the integration constants, the following boundary conditions are applied: At the ends $x = 0$ and $x = 1$, the particle velocity vanishes. Thus at $x = 1$, since the term with $\exp(-k_2 \ell)$ is very small, we have from Equation (10) that

$$C = B \exp(-2ik_G \ell) \tag{11}$$

At $x = 0$, we find

$$D = -i\epsilon(B - C) \tag{12}$$

where

$$\epsilon = \frac{c}{\gamma - 1} \left[ i \frac{C_p}{\omega \chi_G} \right]^{\frac{1}{2}} .$$

Substituting equations for $T_G$ and $T_M$ into Equation (1) and using the condition that $A = T_L = B + C + D$ one finds that

$$B = \frac{\beta I \exp(ik_G \ell)}{2\epsilon \sin k_G \ell [i\omega d C_M + \chi_M k_M - i \chi_G k_2]}$$

At $x = \ell$, the pressure is

$$p_e = \frac{C_p}{a} [B \exp(-ik_G \ell) + C \exp(ik_G \ell)]$$

$$= 2 \frac{C_p}{a} B \exp(-ik_G \ell) .$$

Thus, substituting for $\epsilon$, $k_2$, $k_G$, and a and assuming that $\sin k_G \ell = k_G \ell$ and $(C_p \chi_G)^{\frac{1}{2}} << (C_M \chi_M)^{\frac{1}{2}}$, we find

$$|p_e(\ell)| = \frac{\beta I P_o \chi_G^{\frac{1}{2}} \gamma}{\omega \ell \ .707 \ T_o \ C_p^{\frac{1}{2}}} \left[2 C_M \chi_M + (1.4 C_M d\omega^{\frac{1}{2}})^2 \right.$$

$$\left. + 2.8 C_M d \sqrt{\omega C_M \chi_M}\right]^{-\frac{1}{2}} \qquad (13)$$

Acoustic Ratio

For the rest of the system, we assume that an electrical analogy presented by Morse (1948) will be adequate to obtain the pressure at the microphone. In this analogy, voltage corresponds to the pressure and current corresponds to the total volume gas flow, i.e., particle velocity times cross-sectional area. Each acoustic element contributes differently to the total impedance of the circuit. Figure 2 shows the analog electrical circuit for the system.

$Z_S$ is the acoustic impedance of the sample cavity; it will be considered as a pure compliance (capacitance). $Z_T$ is the acoustic impedance of the connecting tube; it has resistive and inductive components. $Z_M$ is the acoustic impedance of the microphone cavity. The pressure at the microphone diaphragm is then given by

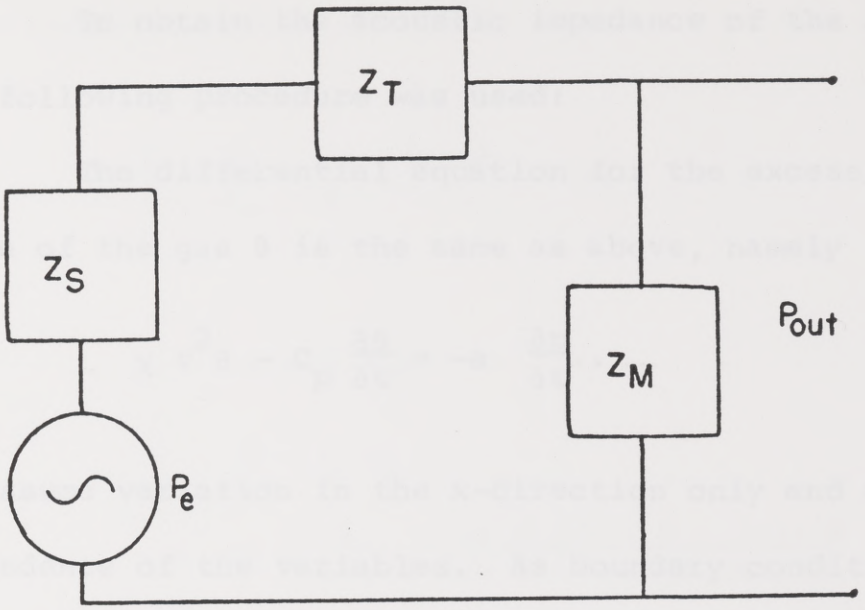


Figure 2. Analog Electrical Circuit.

$$P_{out} = p_e \text{ (acoustic ratio)} = p_e [Z_M/(Z_M + Z_S + Z_T)]$$

Now we define according to Nolle (1953)

$$Z_T = \frac{8\pi\mu\ell}{S^2} + i\omega \frac{4\rho\ell}{3S}$$

where

$\mu$ = viscosity of gas

$\rho$ = density of the gas

$\ell$ = length of tube

S = cross-sectional area of tube

To obtain the acoustic impedance of the cavities, the following procedure was used:

The differential equation for the excess temperature of the gas $\theta$ is the same as above, namely

$$\chi \nabla^2 \theta - C_p \frac{\partial \theta}{\partial t} = -a \frac{\partial p}{\partial t} .$$

We assume variation in the x-direction only and a periodic dependence of the variables. As boundary condition, let $\theta = 0$ at $x = \pm t/2$ where t is the separation between two parallel walls, as shown for microphone cavity in Figure 1.

Thus

$$\theta = \left(1 - \frac{\cos \sqrt{\frac{i\omega C_p}{\chi}}\, x}{\cos \sqrt{\frac{i\omega C_p t^2}{4\chi}}}\right) p_e\, a \exp(-i\omega t)$$

Volume flow is defined as

$$U = -i\omega \left[ P_o^{-1} p_e \exp(-i\omega t)(\text{vol}) - \int_{\text{vol}} \left(\frac{\theta}{T_o}\right) dV \right]$$

and

$$\frac{1}{\text{impedance}} = \frac{U}{p_e \exp(-i\omega t)}$$

From these equations one finds that

$$\frac{1}{Z} = \frac{M\omega}{P_o} - \frac{i\omega}{P_o}\left[\frac{(vol)}{\gamma} - N\right]$$

where

$$M = D\, I_m \Psi$$

$$N = D\, R_e\, \Psi$$

$$\Psi = \frac{1}{1+i}\,\frac{\cos B \tanh B - i \sin B}{i \cos B + \sin B \tanh B}$$

$$B = .707\sqrt{\frac{wC_p t^2}{4\chi}}$$

$$D = 2.83\ (\text{area})\ (1-\tfrac{1}{\gamma})\left(\frac{C_p \omega}{\chi}\right)^{-\frac{1}{2}}$$

Microphone Sensitivity

The sensitivity of the microphone is assumed to be a constant and is given in a 1946 Western Electric brochure as -49.3 db re 1 volt/dyne/cm$^2$ open circuit when biased at 200 volts. Thus

$$Eoc = (3427\ \mu V\ /\text{dyne/cm}^2)\, Pout$$

Electrical Ratio

Electrically the circuit is that shown in Figure 3 and the equivalent circuit is shown in Figure 4. The

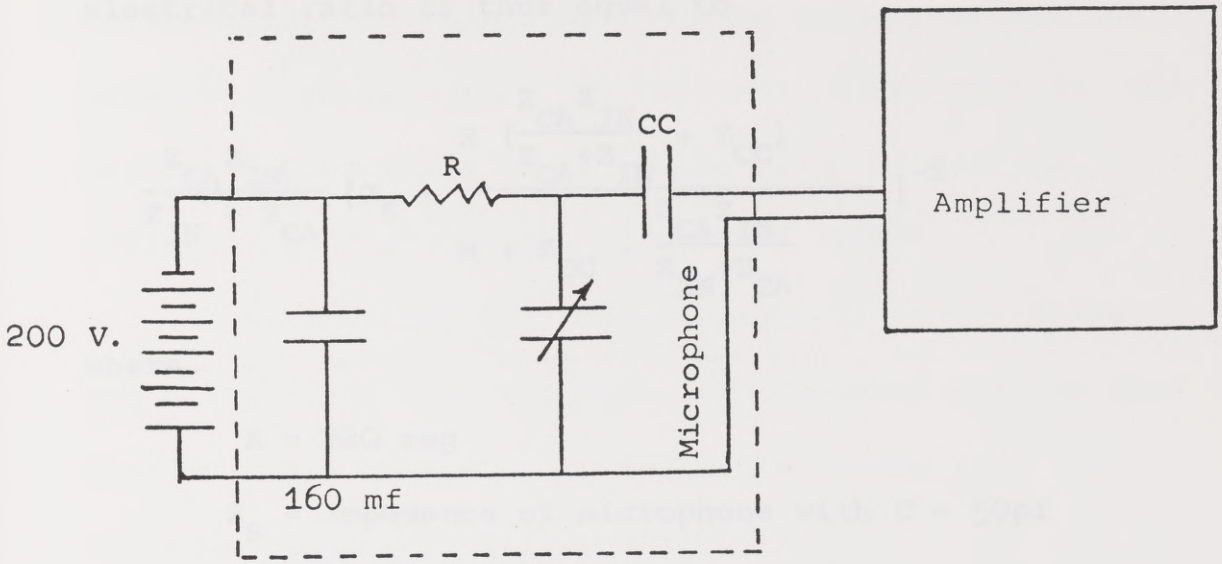


Figure 3. Electrical Circuit.

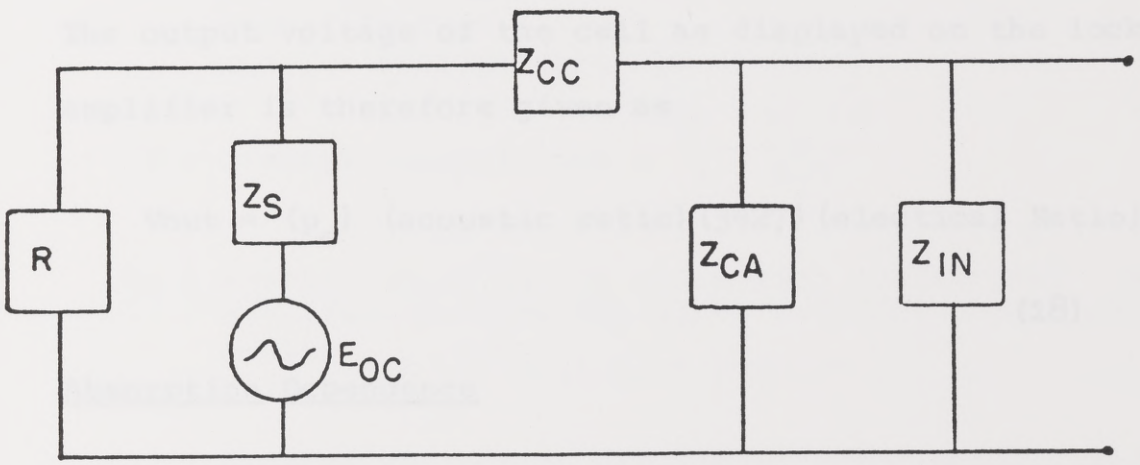


Figure 4. Equivalent Electrical Circuit.

electrical ratio is thus equal to

$$\frac{Z_{CA}Z_{IN}}{Z_{IN}+Z_{CA}}\left[Z_S+\frac{R\left(\frac{Z_{CA}Z_{IN}}{Z_{CA}+Z_{IN}}+Z_{CC}\right)}{R+Z_{CC}+\frac{Z_{CA}Z_{IN}}{Z_{IN}+Z_{CA}}}\right]^{-1}$$

where

$R$ = 220 meg

$Z_S$ = impedance of microphone with C = 50pf

$Z_{CC}$ = impedance of coupling capacitor with C = 4700 pf

$Z_{CA}$ = impedance of cable with C = 90pf

$Z_M$ = input impedance of amplifier = 100 meg

The output voltage of the cell as displayed on the lock-in amplifier is therefore given as

$$V_{out} = (p_e)\ (\text{acoustic ratio})\,(3427)\,(\text{electical Ratio})\,\mu V \qquad (18)$$

Absorption Dependence

The end result after using this technique should, of course, be an absorption spectrum, i.e., how $\alpha$ the optical absorption coefficient changes with wave length.

Accordingly, an attempt must now be made to relate the observed pressure to $\alpha$. To that end, first consider the following discussion based on the study of diffuse reflectivity from powders by Melamed (1963).

Assume that the powder grains of random shape and orientation have the same mean diameter and the surface scatters according to Lambert's cosine law. Now we define some quantities:

$X$ = probability that light emerging from a particle is scattered toward a particle one particle closer to the surface

$$= X_\mu [1 - \{1 - X_\mu (1 + \exp(-\alpha\delta)\} T]^{-1}$$

where $X_\mu$ is taken as .284 the value for close packed spheres
and $\delta$ = average particle diameter

$T$ = average transmission $= \dfrac{(1 - \overline{m_i})M}{1 - \overline{m_i} M}$

$\overline{me}$ = average value of the reflection coefficient from a diffuse surface for light incident from a rare medium $= 2 \int_0^{\pi/2} m(\theta) \sin\theta \cos\theta \, d\theta$

$m(\theta)$ = Fresnel reflection coefficients for unpolarized light

$$= \tfrac{1}{2} \left[\left(\frac{\sin(\theta-\theta')}{\sin(\theta+\theta')}\right]^2 + \tfrac{1}{2}\left[\frac{\tan(\theta-\theta')}{\tan(\theta+\theta')}\right]^2\right.$$

$\theta'$ being the refracted angle.

$\overline{mi}$ = average value of the reflection coefficient from a diffuse surface for light incident from a dense medium

$$= (1 - \sin^2\theta crit) + 2\int_0^{\theta crit} m(\theta)\sin\theta\cos\theta\, d\theta$$

M = total radiation reaching the surface after one pass through a particle

$$= 2\int_0^{\pi/2} \exp(-\alpha\delta\cos\theta)\sin\theta\cos\theta\, d\theta$$

$$= \frac{2}{(\alpha\delta)^2}\left[1 - (\alpha\delta + 1)\exp(-\alpha\delta)\right]$$

In order to obtain the reflectance R of the powder as a whole, Melamed considered a single surface particle; by accounting for all the rays entering and leaving it, he showed that

$$R = 2X\overline{me} + \frac{X(1 - 2X\overline{me})\ T\ (1 - \overline{me}R)}{(1 - \overline{me}R) - (1 - X)(1 - \overline{me})TR}$$

Since for any reasonable thickness of powder there is no light transmitted, the fraction of the incident light energy absorbed ($\beta$) equals 1 - R. Figure 5 shows how $\beta$ depends on $\alpha\delta$ for several different indices of refraction.

The thickness of the absorbing layer (d) also depends on $\alpha$. For small $\alpha$ the layer is several particle

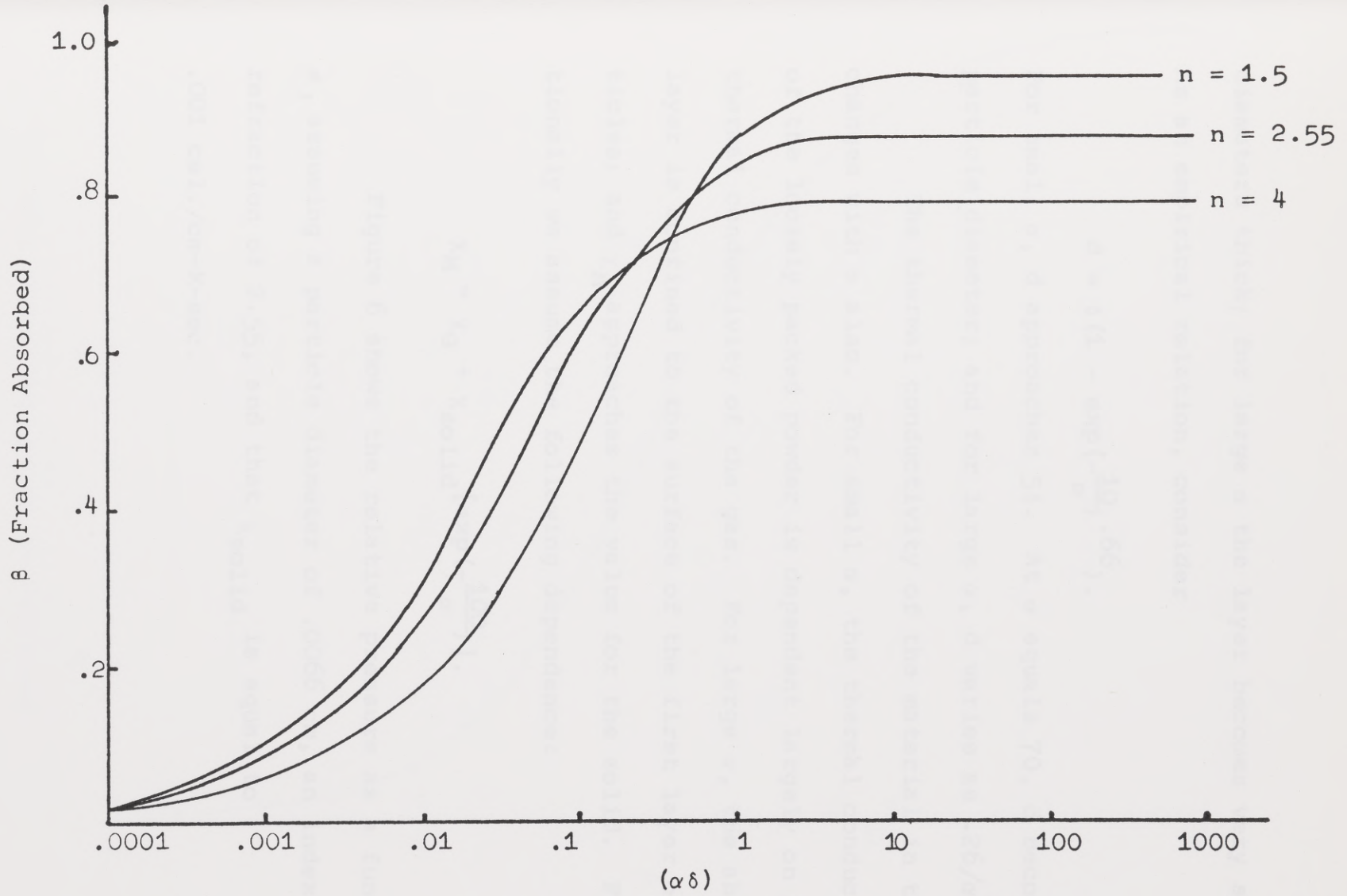


Figure 5. β vs (αδ) for Various n.

diameters thick; for large $\alpha$ the layer becomes very small. As an empirical relation, consider

$$d = \delta(1 - \exp(-\frac{10}{\alpha})^{.66}).$$

For small $\alpha$, d approaches $5\delta$. At $\alpha$ equals 70, d becomes one particle diameter; and for large $\alpha$, d varies as $.26/\alpha^{2/3}$.

The thermal conductivity of the material in the model changes with $\alpha$ also. For small $\alpha$, the thermal conductivity of the loosely packed powder is dependent largely on the thermal conductivity of the gas. For large $\alpha$, the absorbing layer is confined to the surface of the first layer of particles; and $\chi_M$ approaches the value for the solid. Functionally we assume the following dependence:

$$\chi_M = \chi_G + \chi_{solid}[\exp(-\frac{100}{\alpha})].$$

Figure 6 shows the relative pressure as a function of $\alpha$, assuming a particle diameter of .0066 cm, an index of refraction of 2.55, and that $\chi_{solid}$ is equal to .001 cal./cm-K-sec.

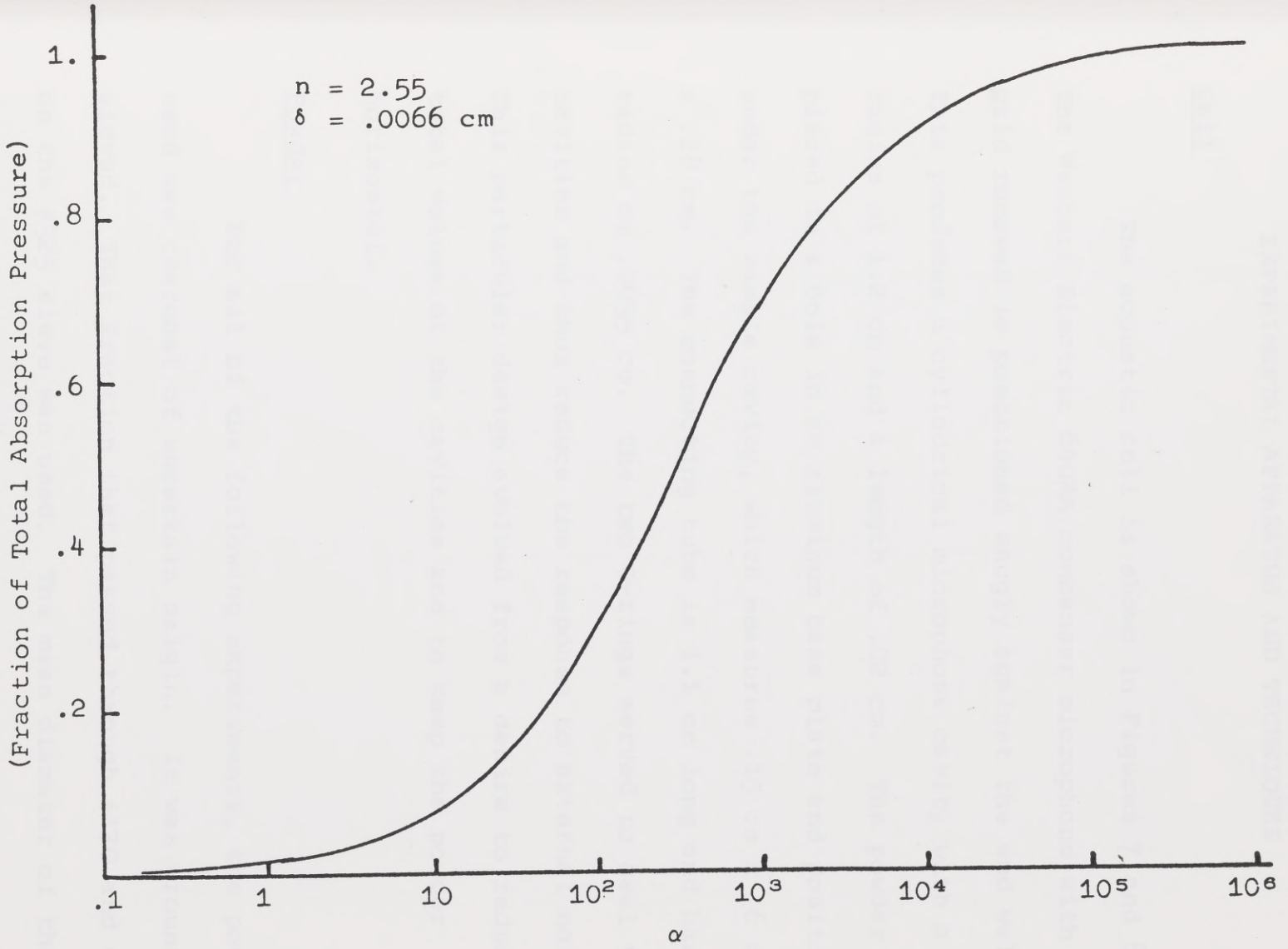


Figure 6. Pressure vs α.

## EXPERIMENTAL APPARATUS AND TECHNIQUES

### Cell

The acoustic cell is shown in Figures 7 and 8. The Western Electric 640AA condenser microphone with the grid removed is positioned snugly against the end wall. This produces a cylindrical microphone cavity with a radius of 1.2 cm and a length of .02 cm. The powder is placed in a hole in an aluminum base plate and positioned under the sample cavity, which measures .15 cm x .6 cm x .28 cm. The connecting tube is 1.1 cm long and has a radius of .0055 cm. The two O-rings served to seal the cavities and thus reduce the response to external noise. This particular design evolved from a desire to reduce the total volume of the cavities and to keep the powder horizontal.

### Powder

For all of the following experiments, the powder used was charcoal of uncertain origin. It was ground and sieved. That fraction that passed through #170 and was on the #325 sieve was used. The mean diameter of the powder grains was taken to be the average of the openings of these sieves or .0066 cm.

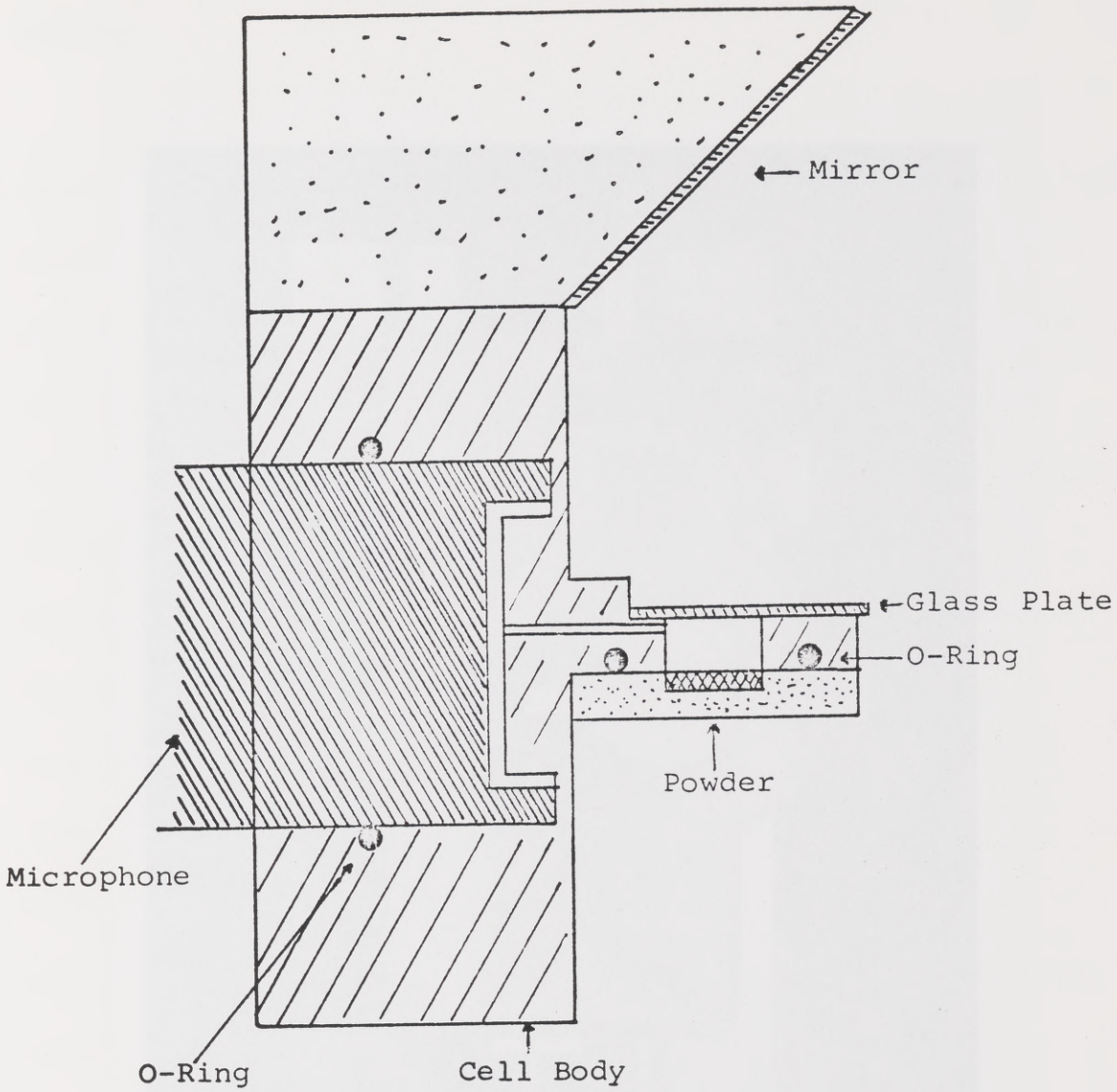


Figure 7. Photoacoustic Cell.

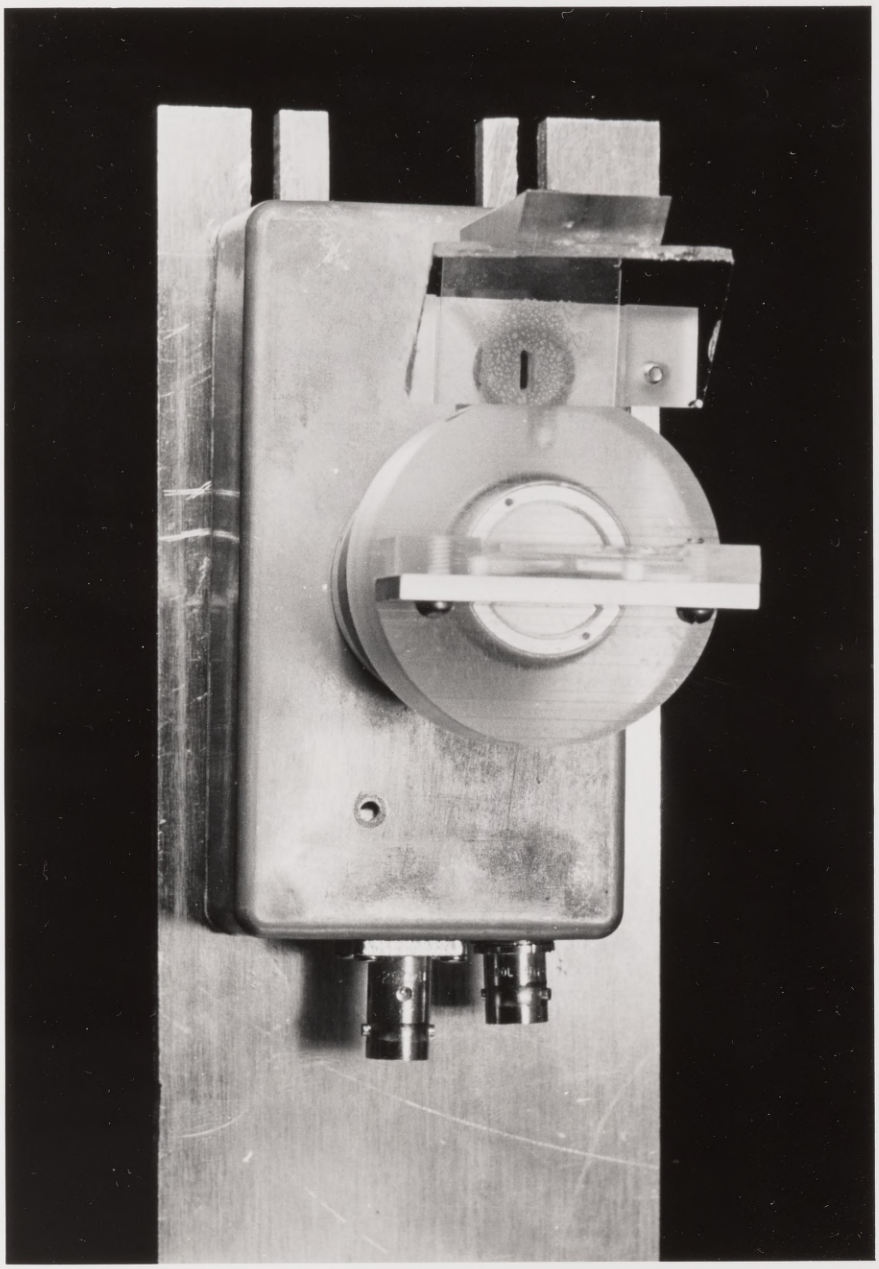

Figure 8. Photograph of Photoacoustic Cell and Mounting.

Optics

The optical system is shown in Figure 9. The lamp is a 3 electrode 75 watt xenon short arc (Illumination Industries X76-2001). The starter is from a Pek 701A power supply and the constant current supply for the lamp was homemade. The chopper is a toothed wheel. For the variable frequency experiment, the wheel was placed on a DC motor combined with a speed regulator; in all other experiments, it was used with an AC synchronous motor. The prism monochrometer is from a Beckman DU Spectrophotometer. All lenses and plates are glass except the first condensing lens which was quartz. To isolate the cell from room noise, it was placed in a 33 cm cube particle board box lined with acoustical tile and loosely surrounded with fiberglass pieces. The box was placed on a 2.5 cm thick fiberglass pad to isolate the cell from table-borne vibration.

Electrical

The electrical circuit was shown in Figure 3 above. Several batteries were connected in series to produce the 200 volt supply. The microphone holder which supported

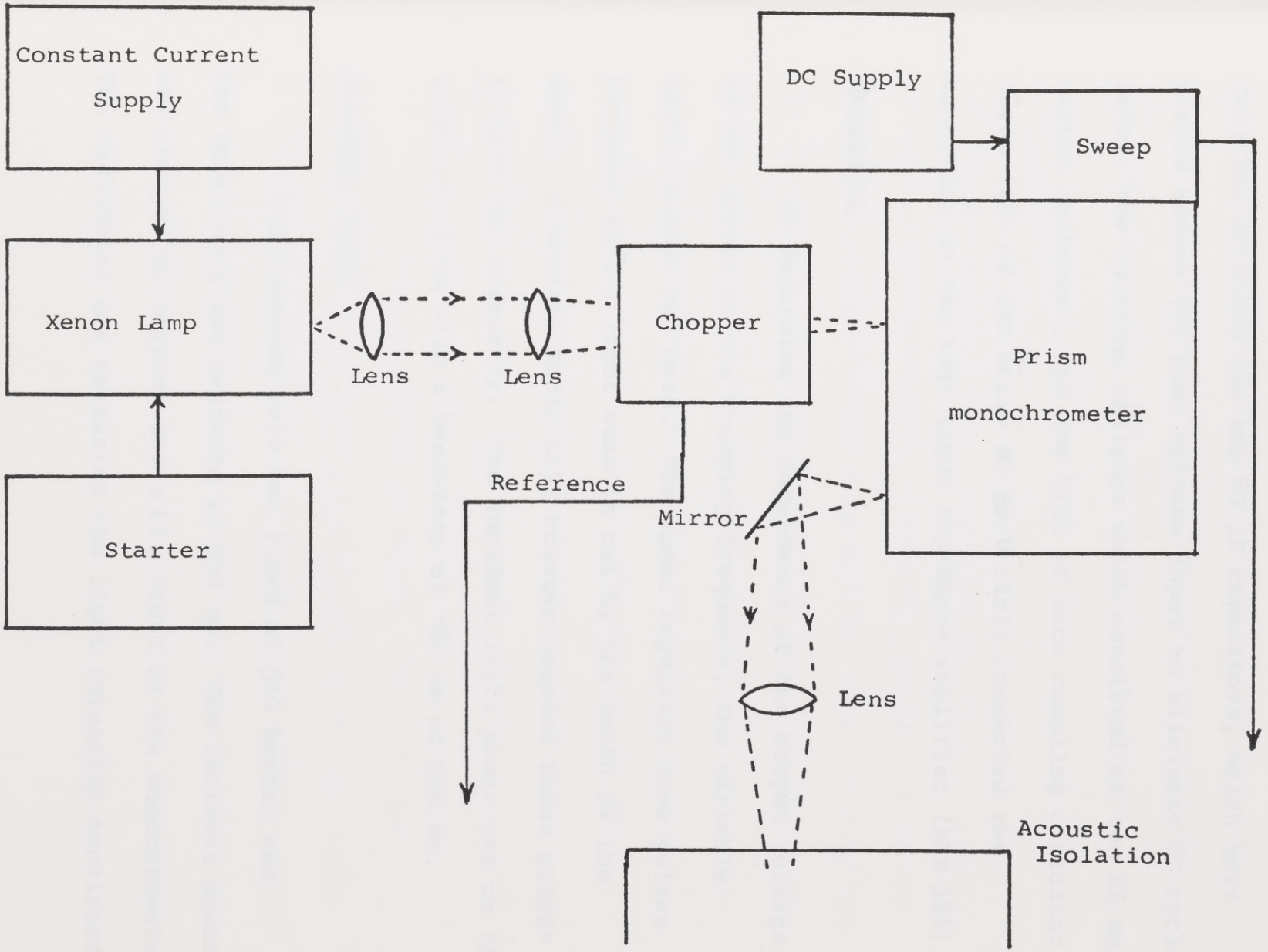


Figure 9. Block Diagram of Optical Arrangement.

the absorption cell was attached to a small metal box. This box shielded the two 80 μF capacitors, which were placed across the bias voltage input to eliminate 60 cycle noise, the charging resistor which consisted of ten 22 meg carbon resistors, and the 4700 pf mica coupling capacitor. Three feet of low noise RG 58/U cable connected the capacitor to the high input impedance amplifier (PAR 124).

Frequency

To determine the dependence of the output voltage of the system on the chopping frequency, the variable speed chopper was used. The speed regulator uses pulses produced when a light beam is cut by the teeth of the wheel. A General Radio 1192 counter counted these pulses to give the frequency. The incident light power was on the order of .5 mw with a bandwidth of ~80 nm at 900 nm.

Incident Power

The chopping rate was fixed at 510 hertz, and the wavelength was centered at 550 nm. The incident power was changed by varying the slit width of the monochrometer. The radiometer for measuring the light intensity consisted

of a GE #412X59 photovoltaic cell into 100 ohms. The voltage across the resistor was read on a 200 mv DPM (Tekelec TA 310-03). This system had previously been calibrated against a TRG 108 ballistic thermopile.

Gas Pressure

The chopping frequency was fixed at 510 hertz. Incident light intensity was on the order of 1.4 mw and the wavelength was centered on 900 nm. The acoustic cell was placed in a glass bell jar which could be pumped out. The pressure in the jar was read on a mercury manometer. In order to equalize the pressure on the microphone diaphragm more quickly, a .012 cm diameter hole was drilled in the front wall of the cell.

Gas

In the same system as above, after the air had been pumped to a pressure of 25μHg, helium was added to the jar to a pressure of 75 cm Hg. The voltage on the PAR was recorded and the helium was pumped out. Argon was then added to a pressure of 75 cm Hg, and the voltage was recorded.

Spectrometer

For the spectrometer the data collection system shown in Figure 10 was added. To obtain a voltage that corresponds to the wavelength, a wire-wound variable resistor was attached to the wavelength dial of the monochrometer. The dial was driven by a stepping motor. The parallel BCD output from the lock-in amplifier and the DVM (Tekelec TA 310-03) goes to an interface (Datos 305-P50E) which supplies the digits serially to the paper tape punch (Roytron Series 500).

The chopping frequency was fixed at 510 hertz. The slit width of the monochrometer was set so as to resolve any structure in the spectra. The incident intensity varied with the wavelength because of the non-linear dispersion of the prism and the characteristics of the xenon arc, but it normally ranged from .01 to .1 milliwatts. The wavelength sweep rate was maintained at about 4 nm/30 seconds by changing the pulse rate of the stepping motor manually.

The time constant of the lock-in amplifier was set at 10 seconds. The Q of the tuned filter section was maintained at 20.

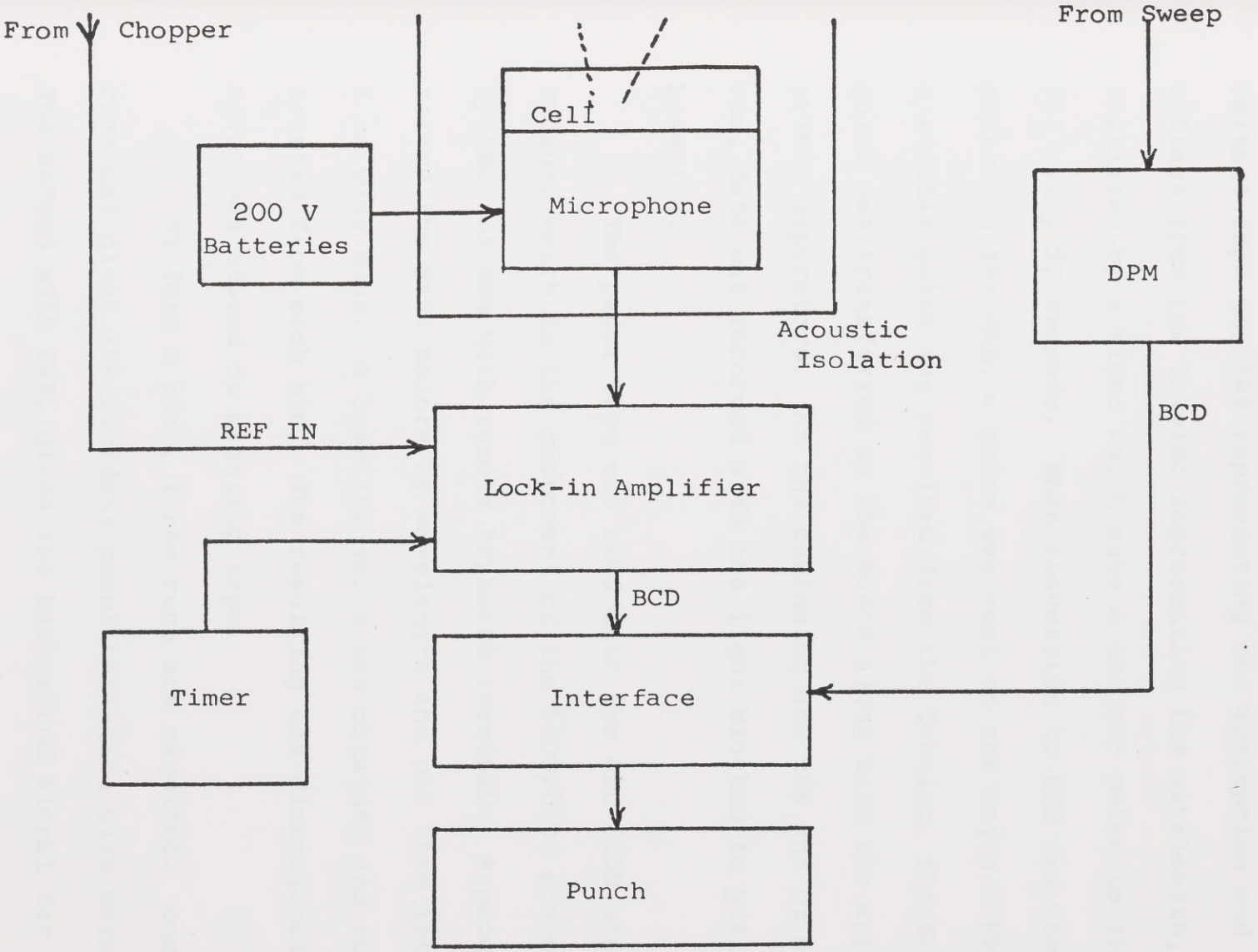


Figure 10. Block Diagram of Data Recording System.

The taking of a data point, which consists of a voltage from the PAR representing the absorption and a voltage from the Tekelec representing the wavelength, was initiated by a timer which gave a trigger pulse to the PAR every 17 seconds. When conversion to BCD was completed in the PAR, a pulse was sent to the Datos. When a similar pulse was received from the Tekelec, the data point was transferred to the punch along with the appropriate separators. At the beginning and the end of a run, data was recorded with the light blocked to yield a baseline.

The paper tape was read into the CDC 6600 via Taurus, which is the component of the 6400/6600 computer system for use with remote keyboard terminals. A program sorted the data points by wavelength and put them into 4 nm wide bins. A baseline value was obtained and subtracted from each bin. The resulting one-dimensional array was stored on magnetic tape.

To form a plot, three runs are required. One with charcoal gives the incident power variation with wavelength. The second with $CaF_2$ gives the background signal for total

reflection, and the third is with the powdered sample. The final result is calculated as

relative absorption = [sample signal - (1 - relative absorption) $CaF_2$ signal]/charcoal signal.

This is normalized to one, smoothed and plotted versus wavelength.

## RESULTS AND DISCUSSION

### Frequency

The frequency dependence is shown in Figure 11. The solid line gives the calculated result from Equation 13 for air and charcoal. The data has been normalized to agree with the calculated result at 70 hertz. The tail off below 30 hertz is a consequence of the very large source impedance of the microphone at low frequencies. The data also shows a change of slope above 500 hertz, a change which is not seen in the calculated line. A possible reason for this change is that above this frequency the period is too short to allow thermal loss to the walls of the sample cavity to occur and so there is a proportionately larger signal. This loss to the walls of the sample cavity is not considered in the above model.

### Incident Light Intensity

The dependence of the output voltage on the incident light intensity is shown in Figure 12. The solid

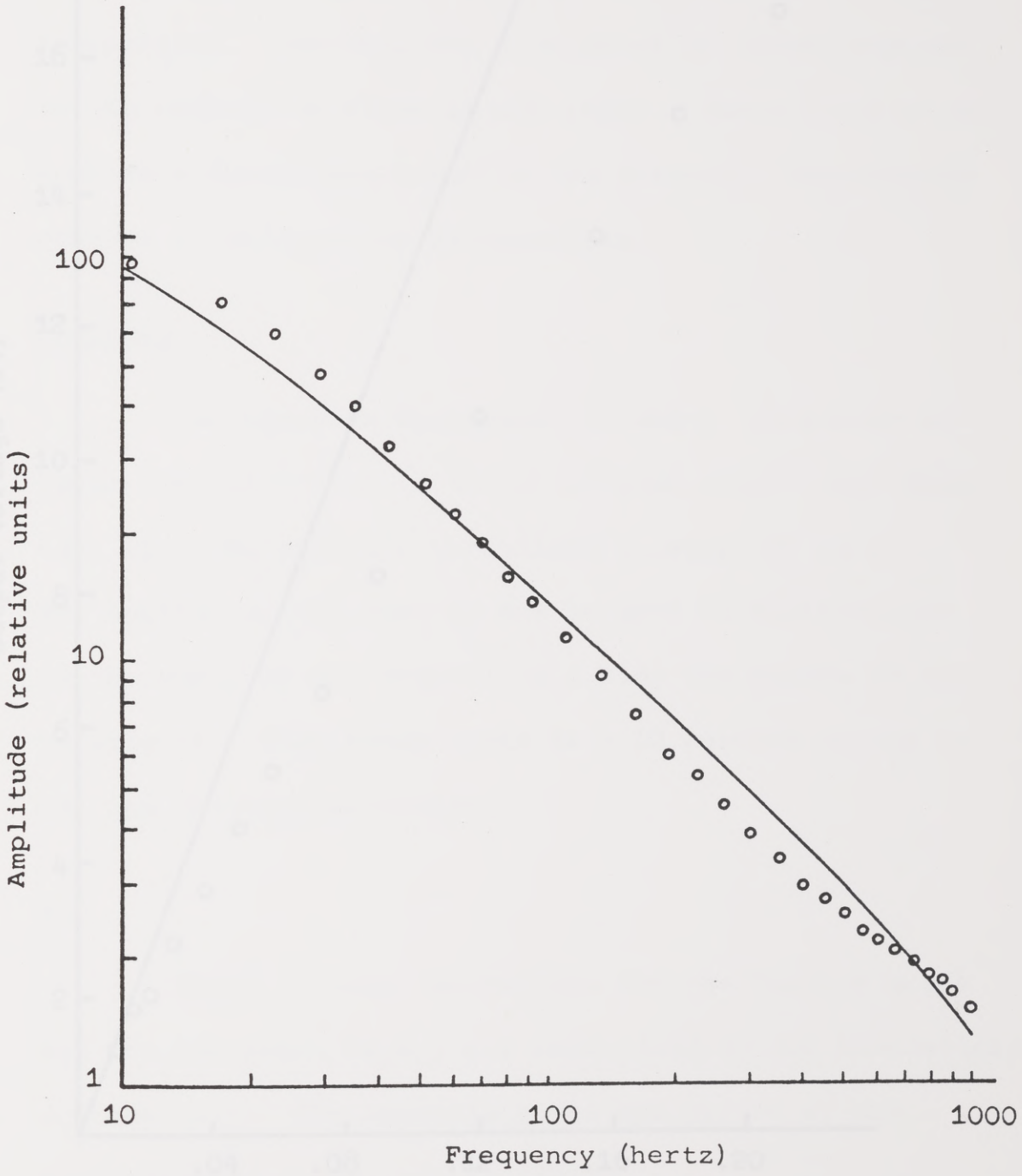


Figure 11. Amplitude vs Frequency. Data normalized to agree with theory at 70 Hz.

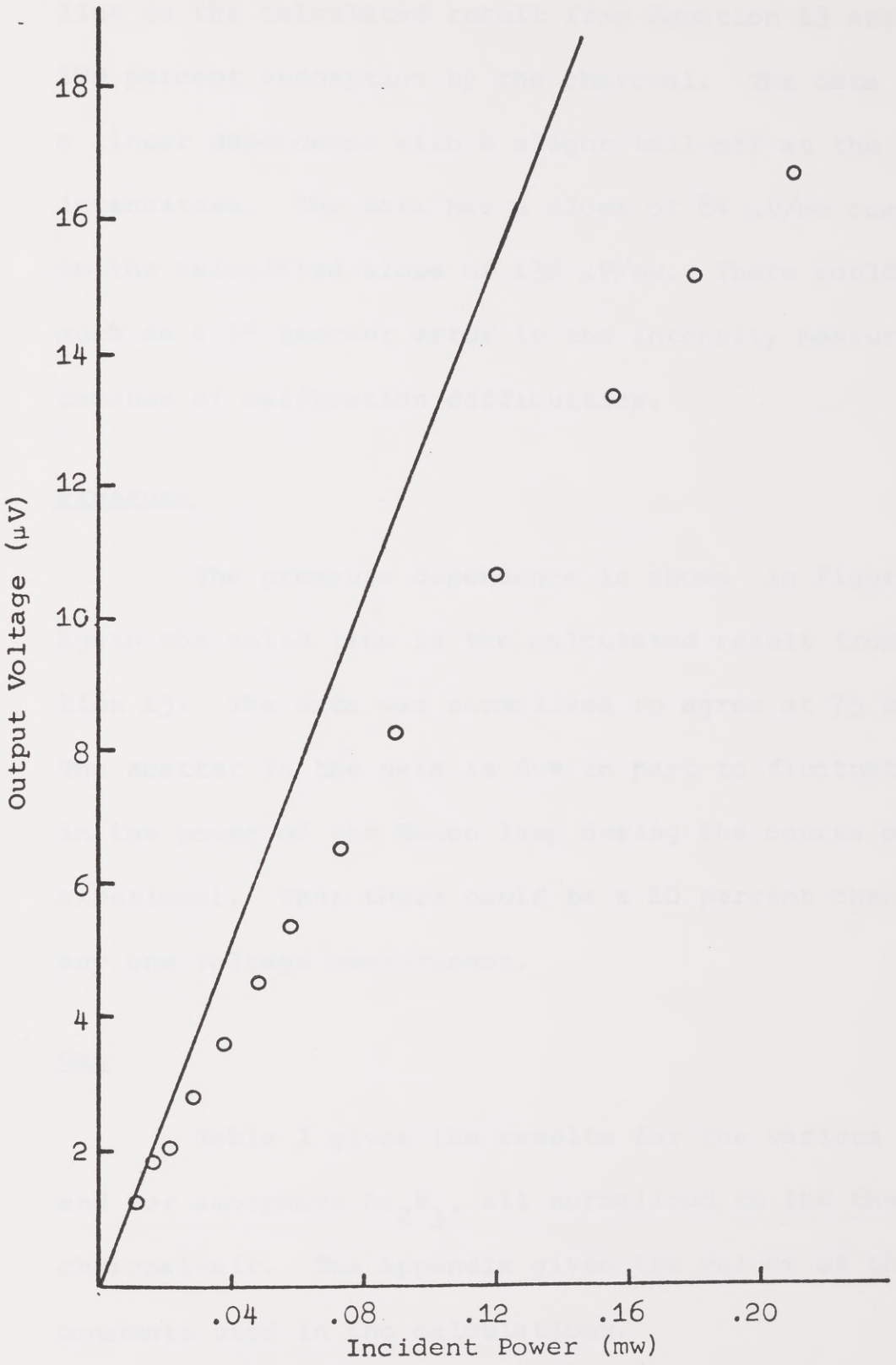


Figure 12. Output Voltage vs Incident Power.

line is the calculated result from Equation 13 assuming 100 percent absorption by the charcoal. The data shows a linear dependence with a slight tail-off at the higher intensities. The data has a slope of 84 μV/mw compared to the calculated slope of 130 μV/mw. There could be as much as a 15 percent error in the intensity measurement because of calibration difficulties.

Pressure

The pressure dependence is shown in Figure 13. Again the solid line is the calculated result from Equation 13. The data was normalized to agree at 75 cm. The scatter in the data is due in part to fluctuations in the power of the Xenon lamp during the course of the experiment. Thus there could be a 10 percent change in any one voltage measurement.

Gas

Table I gives the results for the various gases and for amorphous $As_2S_3$, all normalized to the theoretical charcoal-air. The Appendix gives the values of the constants used in the calculations.

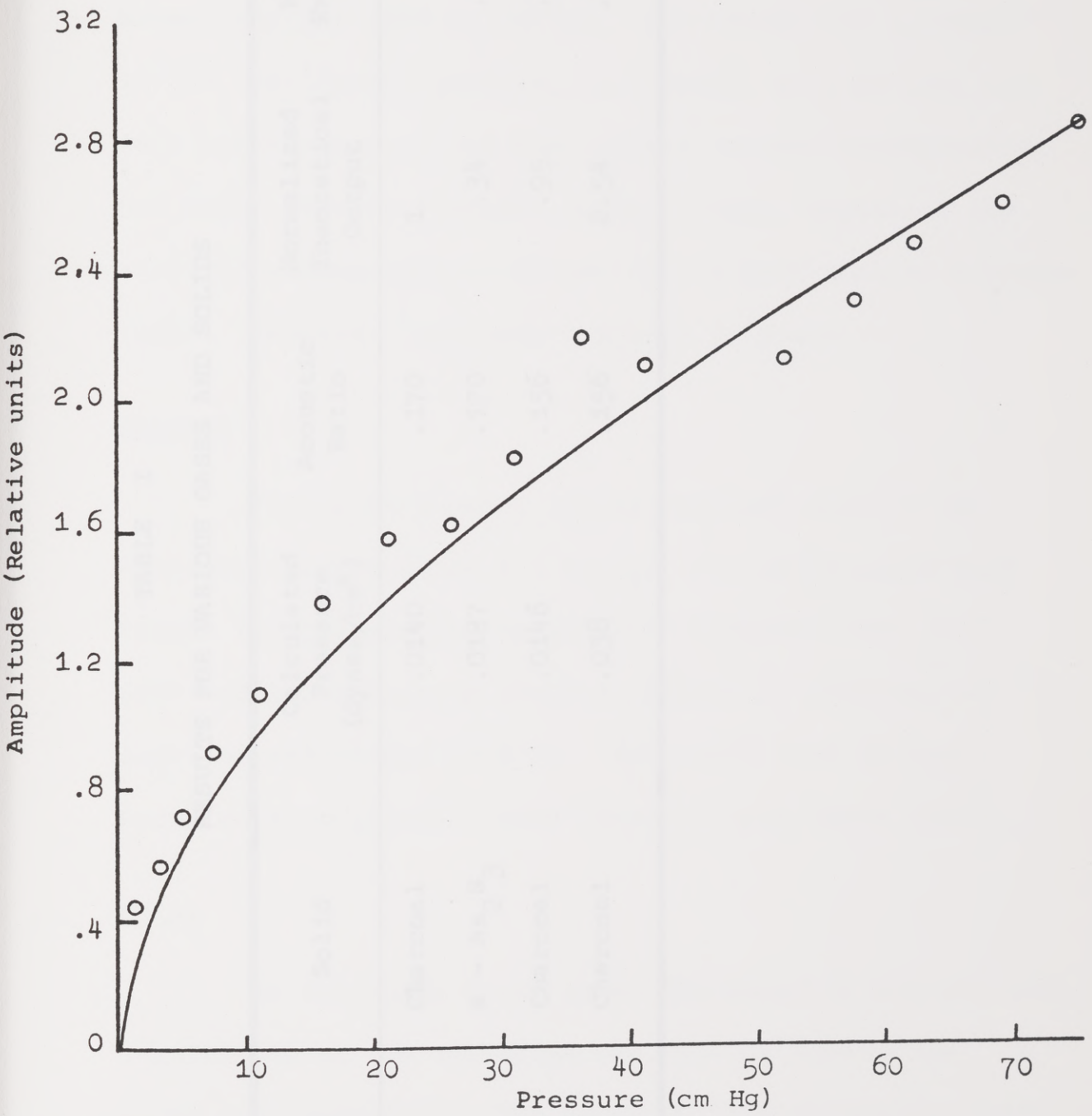


Figure 13. Amplitude vs. Pressure.

TABLE I

RESULTS FOR VARIOUS GASES AND SOLIDS

| Gas | Solid | Calculated Pressure (dynes/$cm^2$) | Acoustic Ratio | Normalized Theoretical Output | Normalized Experimental Result |
|---|---|---|---|---|---|
| Air | Charcoal | .0140 | .170 | 1 | .76 |
| Air | a - $As_2S_3$ | .0127 | .170 | .34 | .36 x .76 |
| Argon | Charcoal | .0146 | .156 | .95 | .91 x .76 |
| Helium | Charcoal | .038 | .156 | 2.54 | .68 x .76 |

As can be seen from the table, there is reasonable agreement between the calculated results and the data except for the case of helium. For helium the increase in the theoretical pressure by a factor of 2.54 over air is a consequence of its much larger thermal conductivity. One might then also expect larger thermal losses to the walls of microphone cavity and thus a much smaller acoustic ratio. However, this does not seem to occur.

Spectra

Figure 14 shows a sample computer plot of the absorption spectra for a - $As_2S_3$. Figure 15 shows some values for the absorption constant obtained from this plot and the theory as shown in Figure 6, assuming an index of refraction of 2.55. The solid line is the accepted experimental curve from Mott and Davis (1971).

Noise

An important point to be discussed is the ultimate sensitivity of the technique and this is limited by noise considerations. The noise in this system can arise from four sources: (1) gas pressure fluctuations,

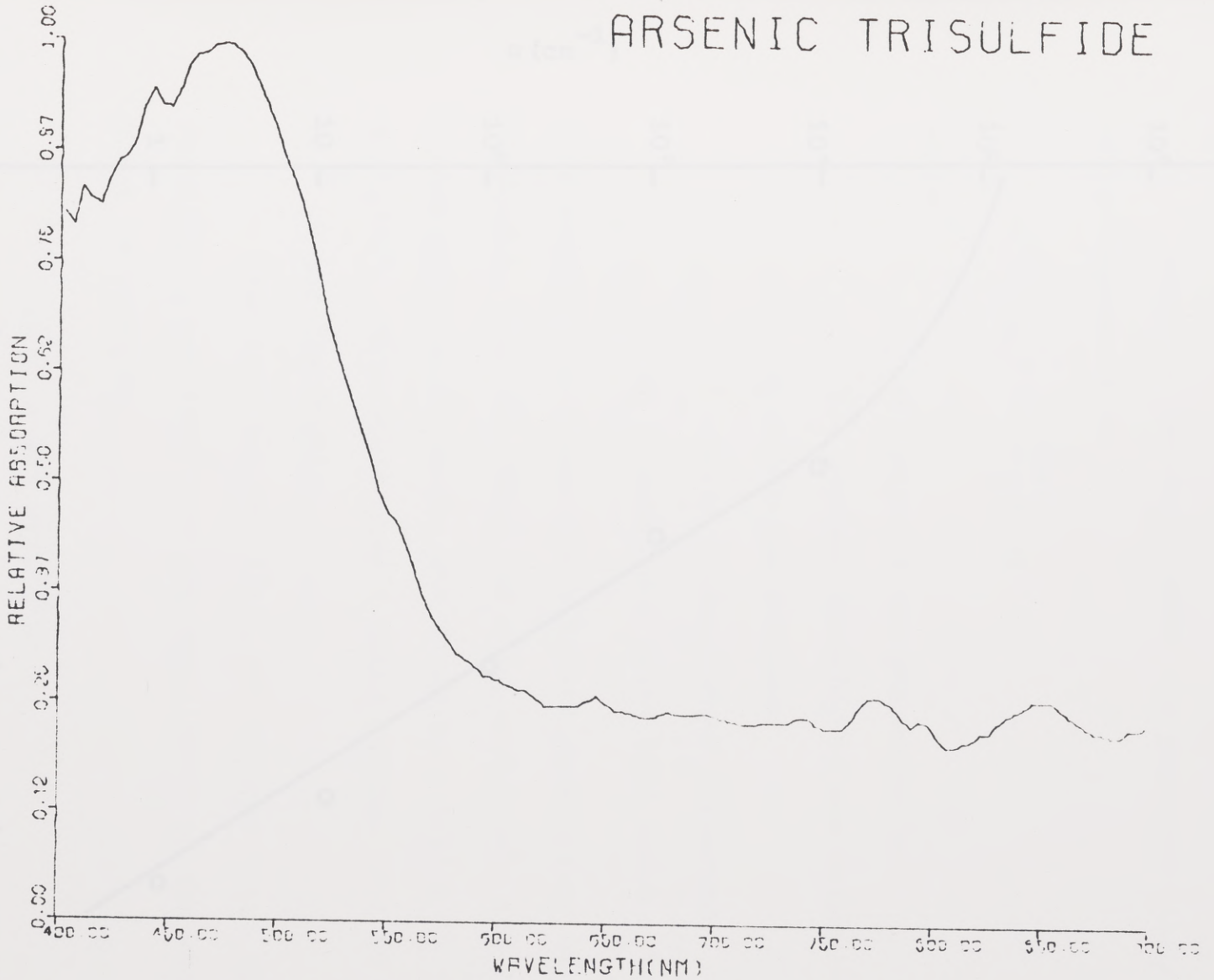


Figure 14. Computer Plot of Absorption Spectra.

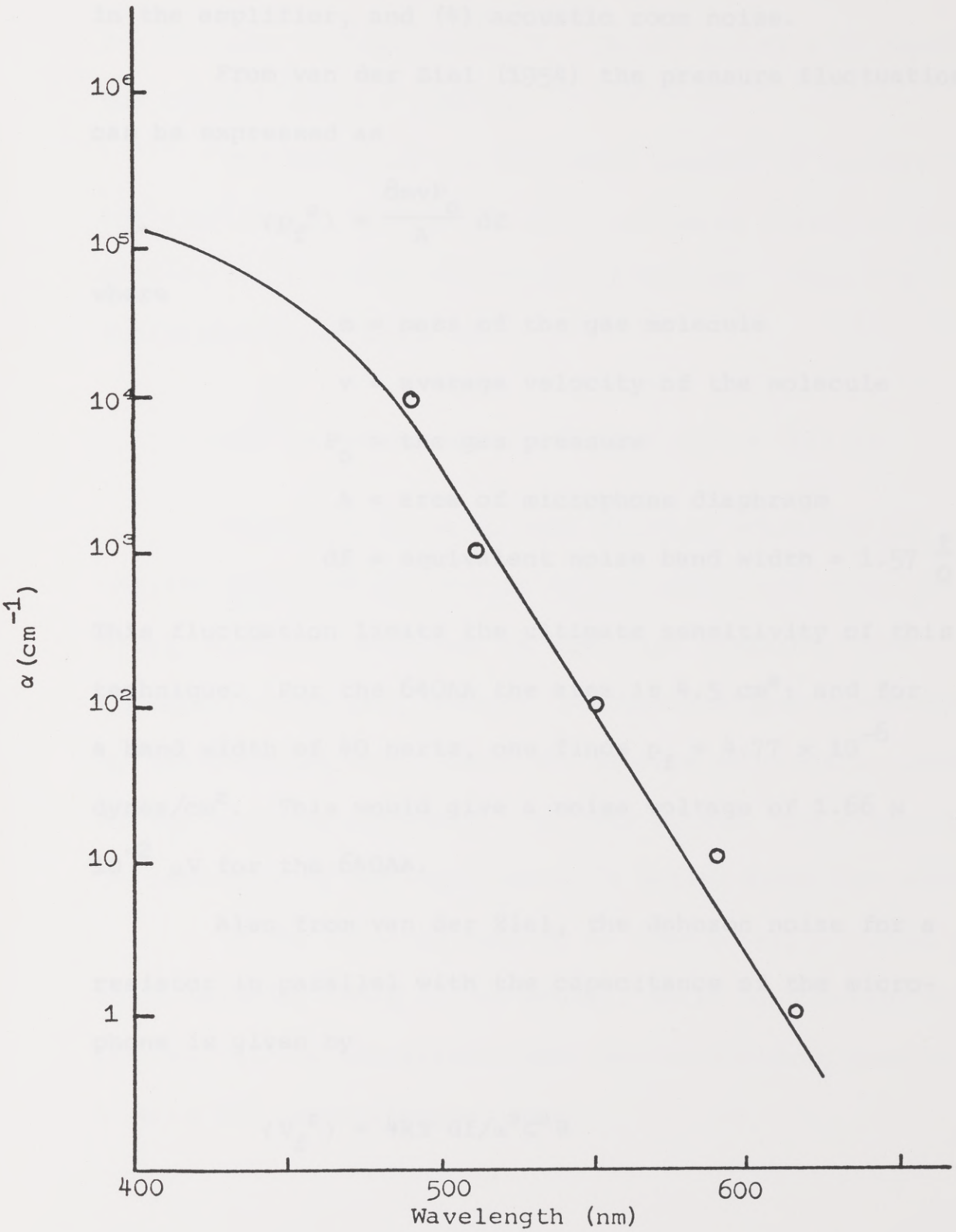


Figure 15. α vs Wavelength.

(2) Johnson noise in the charging resistor, (3) noise in the amplifier, and (4) acoustic room noise.

From van der Ziel (1954) the pressure fluctuations can be expressed as

$$\langle p_f^2 \rangle = \frac{8mvP_o}{A}\, df$$

where

m = mass of the gas molecule

v = average velocity of the molecule

$P_o$ = the gas pressure

A = area of microphone diaphragm

df = equivalent noise band width = $1.57\ \frac{f}{Q}$.

This fluctuation limits the ultimate sensitivity of this technique. For the 640AA the area is 4.5 $cm^2$; and for a band width of 40 hertz, one finds $p_f = 4.77 \times 10^{-6}$ dynes/$cm^2$. This would give a noise voltage of $1.66 \times 10^{-2}$ $\mu V$ for the 640AA.

Also from van der Ziel, the Johnson noise for a resistor in parallel with the capacitance of the microphone is given by

$$\langle V_f^2 \rangle = 4kT\, df/\omega^2 C^2 R$$

where k = Boltzman constant = $1.38 \times 10^{-23}$. With R = 220 meg, f = 510 hertz, C = 50 pf, and df = 40 hertz, the thermal noise = .136 μV.

The noise for the amplifier depends of course, on the amplifier. For the PAR 124, the noise figure is flat at 6 db for a source resistance of 200 meg. Thus the equivalent input noise is

$$10^{\frac{6}{20}} \times \text{source noise} = 1.99 \times .136 = .271 \ \mu V.$$

Most room noise is from building vibration and the air conditioning; and it is generally less than 100 hertz, although there can be some high frequency components. There can, however, be some problems generated by the chopping wheel which may produce an acoustic sound at the chopping frequency. If this occurs, the output may be sensitive to the experimenter's motion about the room.

In the limiting case of no room noise, a signal to noise ratio of unity (.3 μV signal) would be obtained for charcoal-air in the present cell for an incident power of 4 μw at 510 hertz chopping rate.

## CONCLUSIONS

With the spectrometer described above, the major obstacle in the way of obtaining good spectra is the low signal to noise ratio of about 5. Improvements in this system can take several different directions. First the particle size should be known more accurately if precise results for $\alpha$ are desired. To increase the signal, the following improvements are indicated:

(1) The incident light intensity should be increased;

(2) The absorption cell could be redesigned using a smaller diameter microphone as one wall of the sample cavity.

In order to reduce the total noise, the following is suggested:

(1) Reduce the thermal noise produced in the charging resistor by going to a tuned bridge circuit, perhaps similar to that suggested by Zaalberg van Zelst (1967).

(2) Redesign the chopping wheel to be silent.

The data suggests that the parameters to use for the largest signal to noise ratio, at least for the present design, are air at atmospheric pressure and a

chopping frequency of at least 1000 hertz and perhaps higher.

In general, this study has shown that the photoacoustic technique can give an accurate absorption spectrum for $\alpha$ in the range $.5 < \alpha < 2 \times 10^5$. Outside this range, the pressure change is less than one percent. The ultimate resolution is dependent on the magnitude of the signal voltage and is only limited by the statistical pressure fluctuations. Furthermore, the theory described above does account for the main features of the technique and should be an aid in choosing the optimal parameters for further use of this technique.

# APPENDIX

## APPENDIX

### CONSTANTS USED IN THE CALCULATIONS

| Solids | Density (g/cc) | $\beta$ | $\chi$solid (cal/cm-K-sec) | Specific Heat cal/K-gm | $C_M$ ($\rho Cp$) |
|---|---|---|---|---|---|
| Charcoal | .35 | 1 | .001 | .16 | .056 |
| a - $As_2S_3$ | 3.43 | .875 | * | .113 | .388 |

*Assumed to be same as $As_2Se_3$ - $As_2Te_3$ series--.001.

| Gases | $\rho$ (g/cc) | $\chi_G$ (cal/cm-K-secx$10^5$) | $\gamma$ | $\mu$ (micropoises) | $Cp_s$ (cal/cm x $10^4$) |
|---|---|---|---|---|---|
| Air | .0013 | 5.48 | 1.402 | 182 | 2.8 |
| Helium | .000178 | 33.9 | 1.63 | 196 | 2.28 |
| Argon | .00178 | 4.05 | 1.648 | 226 | 2.1 |

# REFERENCES

# REFERENCES


Beranek, L. L. (1949)
Acoustic Measurements, Wiley.

Golay, M. J. E. (1947)
The Review of Scientific Instruments, 18, 347.

Hunter, J. L. (1957)
Acoustics, Prentice-Hall.

Kreuzer, L. B. (1971)
Journal of Applied Physics, 42, 2934.

Melamed, N. T. (1963)
Journal of Applied Physics, 34, 560.

Morse, P. M. (1948)
Vibration and Sound, McGraw-Hill.

Mott, N. F. and E. A. Davis (1971)
Electronic Processes in Non-crystalline Materials,
Clarendon Press.

Nolle, A. W. (1953)
The Journal of the Acoustical Society of America, 25,
32.

Parker, J. G. (1973)
Applied Optics, 12, 2474.

Rosencwaig, A. (March 1973)
Bulletin of the American Physical Society, 18, 357.

_____. (April 1973)
Optics Communications, 7, 305.

_____. (August 1973)
Science, 181, 657.

van der Ziel, A. (1954)
Noise, Prentice-Hall.

Zaalberg van Zelst, J. J. (1947)
Philips Technical Review, 9, 357.

The vita has been removed from the digitized version of this document.